Available online at www.sciencedirect.com
ScienceDirect
Polymer 48 (2007) 5713–5720
polymer
www.elsevier.com/locate/polymer

Real-time observation of coil-to-globule transition in thermosensitive poly(*N*-isopropylacrylamide) brushes by quartz crystal microbalance

Masahiko Annaka [a,*], Chie Yahiro [a], Kenichi Nagase [b], Akihiko Kikuchi [c], Teruo Okano [b]

[a] *Department of Chemistry, Kyushu University, Fukuoka 812-8581, Japan*
[b] *Institute of Advanced Biomedical Engineering and Science, Tokyo Women's Medical University, Tokyo 162-8666, Japan*
[c] *Department of Material Science and Technology, Tokyo University of Science, Chiba 278-8510, Japan*

Received 10 March 2007; received in revised form 16 June 2007; accepted 26 June 2007
Available online 6 July 2007

Abstract

Thermosensitive poly(*N*-isopropylacrylamide) (PNIPAm) brushes grafted on SiO_2-coated quartz crystal surface were prepared by the surface initiated radical polymerization. Using X-ray photoelectron spectroscopy (XPS) and atomic force microscopy (AFM), about 50 nm thickness of PNIPAm brushes were successfully formed. Quartz crystal microbalance with dissipation (QCM-D) is employed to investigate the collapse and swelling behavior of the PNIPAm brushes in water in real time. Both frequency and dissipation of PNIPAm layer were found to change gradually over the temperature range 15–50 °C, indicating that the brushes undergo a continuous transition. This continuous change is attributed to the nonuniformity and stretching of PNIPAm brushes as well as the cooperativity between collapse and dehydration transition.
© 2007 Elsevier Ltd. All rights reserved.

Keywords: Poly(*N*-isopropylacrylamide); Polymer brush; Coil-to-globule transition

1. Introduction

The behavior of polymer molecules when one of their ends is tethered to a surface or an interface is qualitatively different from that of chain molecules in bulk. The presence of a wall limits the configurational space of the chain and the two-dimensional anchoring makes the repulsions between neighboring chains different from that of polymers in bulk. The study of tethered layers extends to many fields, including chemistry, physics, and material science. During the last two decades many scientists have investigated the behavior of tethered layers using experimental and theoretical methodologies. On the experimental side, the measurements of the force–distance profiles have provided very valuable information on how the modified surfaces interact with each other [1–4]. Scattering methods have been applied to elucidate the structure of the layers through the monomer density profiles as a function of the distance from the tethering surface and how this structural property changes with the quality of solvent [5–10]. On the theoretical side, there are scaling approaches [11–21], self-consistent field (SCF) calculations [22–24], and computer simulations including molecular dynamics (MD) [25–27] and Monte Carlo (MC) [27–29] methodologies.

Polymer chains grafted onto a surface form a polymeric brush when the grafting density is high enough that the chains have to stretch outward from the surface without any overlapping in good solvent due to the effect of exclusion [13,30,31]. Such a coil-to-brush transition has attracted much interest with various implications [32–38]. The properties of polymer brushes are different from those of flexible polymer chains in solution where chains adopt random coil configurations. It has been theoretically predicted that the collapse of the surface-grafted polymer brushes accompanying a solubility transition proceeds continuously as the solvent quality decreases [20,33]. This effect becomes more pronounced with decrease

* Corresponding author. Tel.: +81 92 642 2594; fax: +81 92 642 2607.
E-mail address: annaka-scc@mbox.nc.kyushu-u.ac.jp (M. Annaka).

0032-3861/$ - see front matter © 2007 Elsevier Ltd. All rights reserved.
doi:10.1016/j.polymer.2007.06.067

in effective dimensionality [20]. Experimental results obtained for poly(*N*-isopropylacrylamide) (PNIPAm) grafted on spherical nanoparticles and from other polymer brushes systems have borne out this prediction [39,40].

PNIPAm is well known to exhibit LCST-type phase behavior in water, namely PNIPAm chain swells with random coil conformation at lower temperatures, and collapses into globule when the solution temperature is above LCST [41–43]. When PNIPAm is grafted to a solid surface, the resulting surface shows temperature-dependent surface properties, such as wettability [44,45] and film thickness [46]. This property has been cleverly utilized in number of applications, including chromatography [47–51] and mammalian cell release surfaces [52,53].

While the phase transition of free PNIPAm chains in aqueous solution has been extensively studied, the phase behavior of PNIPAm chains grafted to a solid surface is less explored. Surface plasmon resonance measurements by Lopez and coworkers [54] and neutron reflectivity studies by Kent and coworkers [55–57], revealed that phase transition of PNIPAm brushes take place over a broad temperature range around 32 °C. By using quartz crystal microbalance (QCM), Zhang et al. [58,59] showed that the pancake-to-brush transition of thiol-terminated PNIPAm chains on gold surface also was gradual. Recently study by Genzer and coworkers [60] confirmed that such a broad transition of PNIPAm brushes is induced by salt.

Most investigations of transitions for surface-grafted PNIPAm on planar surface have employed contact angle measurements, which typically show a sharp transition for surface-grafted PNIPAm chains at about 32 °C [44,45]. Force versus distance curves measured by atomic force microscopy (AFM) have shown reduced steric repulsion on increasing temperature from below the LCST to above the LCST [46,61]. These results suggest that the outer layer of grafted PNIPAm chains rapidly respond to temperature change. Typically these measurements have been carried out only at two temperatures, one below and one above the LCST.

To our knowledge, a few systematic studies have been reported on the collapse of PNIPAm brushes as a function of temperature and/or in real time. In this study, real-time observation of thermally-induced transition of PNIPAm brushes are investigated by using quartz crystal microbalance with dissipation measurements (QCM-D). QCM probes a combination of the acoustic impedance and thickness, which can be termed the ''acoustic moment''. Importantly, the QCM is sensitive to any adsorbed mass, including solvent, associated with the films. In addition, QCM-D technique provides information not only on the behavior of outer layer of the brushes, but on inside the layer, and hence on the viscoelastic properties of brushes.

2. Experimental

2.1. Materials

N-isopropylacrylamide (NIPAm, Kojin Co.) was recrystallized in toluene/*n*-hexane mixture three times. 4,4′-Azobis(4-cyanovaleric acid) (ABCA, Acros Organics), 3-(aminopropyl)triethoxysilane (APTES, Shinetsu Chemical), and dicyclohexylcarbodiimide (DCC, Wako Pure Chemical) were used as received. Toluene (Kanto Chemical), *N*,*N*-dimethylformamide (DMF, Kanto Chemical), and ethanol (Kanto Chemical) were distilled over drying agent under dry nitrogen atmosphere prior to use.

2.2. Graft polymerization of NIPAm onto a crystal surface

The SiO_2-coated quartz crystal surface was cleaned using $H_2O/H_2O_2/NH_4OH$ (5:1:1 in volume) solution at 80 °C for 15 min, and then rinsed with deionized water. The crystal surface was further cleaned with 0.1 N HCl, followed by rinsing with deionized water.

Several wash–dry cycles were performed until concordant frequencies were obtained. The crystal surface was dried under a stream of N_2 gas.

The pre-treated crystal was placed into a 70 mL toluene solution containing 2 mL of APTMS and refluxed under N_2 atmosphere for 24 h (Scheme 1). When the silanization was complete, the crystal surface was rinsed successively with toluene, ethanol, and acetone, and finally dried under a stream of N_2 gas. The APTMS modified surface was then exposed to 70 mL solution of DMF containing 0.35 g of ABCA, 3.5 g of DCC, and 87 μL of pyridine as catalyst at 35 °C for 24 h to introduce the initiator (ABCA) on the SiO_2 surface.

For the surface initiated graft polymerization with NIPAm, the initiator modified crystal was immersed in a 70 mL of ethanol solution containing 10.5 g of NIPAm with one side covered with a protective casing made of Teflon. After deaeration of the system by bubbling N_2 gas, the graft polymerization was carried out at 70 °C for 16 h under N_2 atmosphere. The quartz crystal grafted with PNIPAm was rinsed successively with toluene, ethanol and deionized water to remove the PNIPAm chains physically absorbed on the grafting layer.

The apparent molecular weight of PNIPAm chains grafted on the SiO_2 surface was determined to be $M_n = 23{,}800$ by gel permeation chromatography for the nonattached PNIPAm chains free in solution [62]. The polydispersity of PNIPAm was evaluated to be $M_w/M_n \approx 1.5$.

2.3. Characterization of the surface

The PNIPAm-modified crystal surface is characterized by X-ray photoelectron spectroscopy (XPS), and atomic force microscopy (AFM) measurements. XPS analysis was performed on an AXIS-165 X-ray photoelectron spectrometer (Shimazu/Kratos).

The PNIPAm-modified crystal surface is characterized by contact-mode AFM analysis, carried out using SPA 400 scanning probe micro systems (Seiko Instruments Inc.). The images were acquired in solution with silicon nitride tips with spring constant of 0.75 $N\,m^{-1}$.

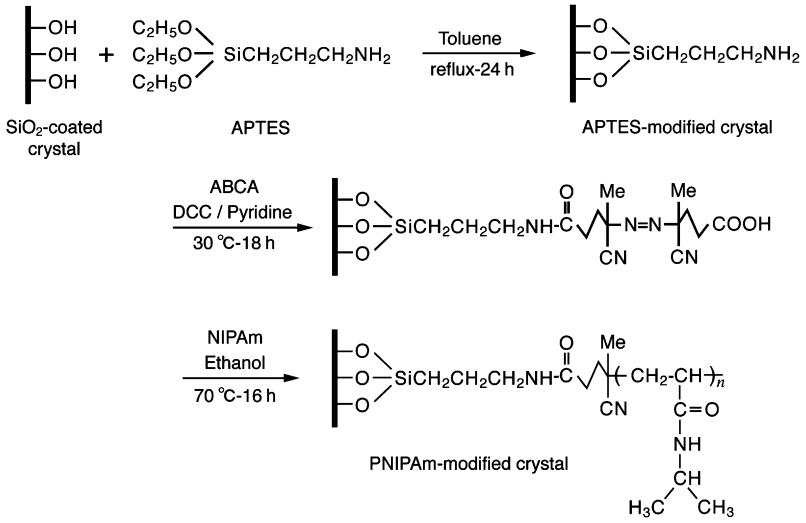

Scheme 1. Preparation of PNIPAm brush on SiO_2-coated quartz crystal for QCM-D.

2.4. Quartz crystal microbalance

Quartz crystal microbalance (QCM Z-500) having an AT-cut quartz crystal with fundamental resonant frequency of 5 MHz and a diameter of 14 mm is from KSV Instruments, Finland. This instrument allows the simultaneous measurements of changes in resonance frequency f and dissipation energy D. The energy dissipation is measured on the basis of the principle that when the driving power to a piezoelectric oscillator is switched off, the voltage over the crystal decays exponentially and a damped oscillating signal is recorded [63,64]. Hence, before disconnection of the diving oscillator, we obtain f and D is obtained after the disconnection. The dissipation factor is defined as

$$\Delta D = \frac{E_{\text{dissipated}}}{2\pi E_{\text{stored}}} \tag{1}$$

where $E_{\text{dissipated}}$ is the energy dissipated during one oscillation, and E_{stored} is the energy stored in the oscillating system. Any mass Δm, deposited on one or both of the electrodes of a crystal, induces a shift in the frequency Δf that is proportional to the added mass. If the mass is deposited evenly over the electrode(s), and if Δm is much smaller than the mass of the crystal itself, the frequency shift is related to the adsorbed mass by Sauerbery equation [65]

$$\Delta m = -\frac{\rho_q t_q}{f_0}\frac{\Delta f}{n} = -\frac{\rho_q \nu_q}{2f_0^2}\frac{\Delta f}{n} = -\frac{C\Delta f}{n} \tag{2}$$

where ρ_q and ν_q are specific density and shear wave velocity in quartz, respectively, t_q is the thickness of the quartz crystal, n is the overtone number, and f_0 is the fundamental resonance frequency ($n = 1$). In this study the value of the constant C is 17.7 ng cm^{-2} Hz^{-1}. The frequency shift is measurable to within ± 1 Hz in aqueous medium, and the temperature was controlled within a range of ± 0.01 °C by custom-made temperature controller with a Peltier element. We collected frequency (f) and dissipation (D) values of quartz crystal in two modes, in quasi-static mode and in real-time mode. In quasi-static mode, the response curve was collected at discrete temperature intervals. The data was collected at the point where frequency attained a constant value at each temperature; i.e., the fluctuation of frequency is within ± 2 Hz. In real-time mode, the temperature of water was changed continuously at constant rate. Δf and ΔD values from the fundamental were usually noisy because of insufficient energy trapping and therefore discarded [66,67].

3. Results and discussion

3.1. Atomic force microscopy

To get quantitative and detailed impression of the surface morphology, AFM images of three substrates, (a) SiO_2-coated crystal, (b) APTES-modified crystal, and (c) PNIPAm-modified crystal, were taken. The AFM image of SiO_2-coated crystal shows a relatively smooth surface, and its surface roughness is less than 1 nm as shown in Fig. 1a. From the AFM image for the APTES-modified crystal surface (Fig. 1b), the silane molecules are densely arrayed, and the thickness of APTES monolayer is about 3 nm. The thickness of the PNIPAm-modified layer is about 50 nm (Fig. 1c). It is, however, seen that the surface exhibits, in addition to ordered arrangement of the polymers, a surface corrugation due to the aggregation of PNIPAm chains.

3.2. X-ray photoelectron spectroscopy

To investigate the composition of the surface, XPS measurement was employed. Fig. 2 shows C1s, N1s, and N1s spectra for (1) the SiO_2-coated crystal, (2) APTES-modified crystal, and (3) PNIPAm-modified crystal. Fig. 1a exhibits the C1s signals. For the SiO_2-coated crystal, the presence of the C1s signal is attributed to the interference of unavoidable

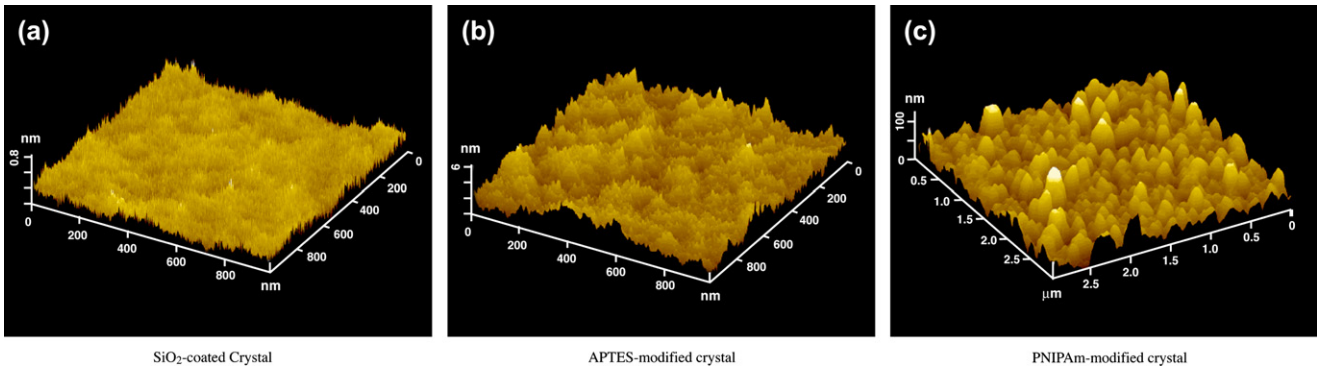

Fig. 1. AFM three-dimensional images of (a) SiO_2-coated crystal, (b) APTES-modified crystal, and (c) PNIPAm-modified crystal.

pollution, and the signal is weak. After the silane treatment, the C1s signal intensity at 285 eV was enhanced largely. For the PNIPAm-modified crystal, three peaks are resolved by the careful peak fitting on the C1s signal, which correspond to different carbons in PNIPAm: (i) aliphatic hydrocarbon for C–C/C–H at the binding energy of 285 eV, (ii) acylamino carbon C–N at 286 eV, and carbonyl carbon C=O at 289 eV. These three signals indicate the presence of PNIPAm on the crystal surface. From Fig. 1b, for the SiO_2-coated crystal, no signal was detected. After the silane treatment, the appearance of the N1s signal at 399 eV indicates that the APTES monolayer was introduced to the SiO_2-coated crystal surface through a covalent bond. For the PNIPAm-modified crystal, new N1s signal appeared at 401 eV, which is attributed to the acylamino nitrogen N–C=O of the PNIPAm chain. Fig. 2c depicts the O1s spectra for three substrates. The O1s signal of SiO_2-coated crystal is almost same as that of APTES-modified crystal, both spectra exhibit the O1s signals of the O–Si bond at 532 eV. As for the O1s signal of the PNIPAm-modified crystal, additional signal was observed at 534 eV corresponding to the carbonyl oxygen O=C of PNIPAm. The wide scan XPS analysis indicates that PNIPAm brushes are generated on the SiO_2-coated crystal surface by the method given in Scheme 1.

3.3. Quartz crystal microbalance

Since the response of the quartz crystal is affected by variation in temperature, viscosity, and the density of the medium above the sensor surface, the inherent crystal effects must be taken into consideration to obtain the true response of the PNIPAm brushes. First Δf and ΔD are measured for SiO_2-coated crystal at different temperatures.

In a Newtonian liquid, the frequency response of a quartz crystal can be quantitatively described by the Kanazawa–Gordon relation [68]

$$\Delta f = -n^{1/2} f_0^{3/2} \left(\eta_1 \rho_1 / \pi \mu_q \rho_q\right)^{1/2} \tag{3}$$

where ρ_q and μ_q are the density and shear modulus of quartz, and ρ_1 and η_1 are the density and viscosity of the liquid

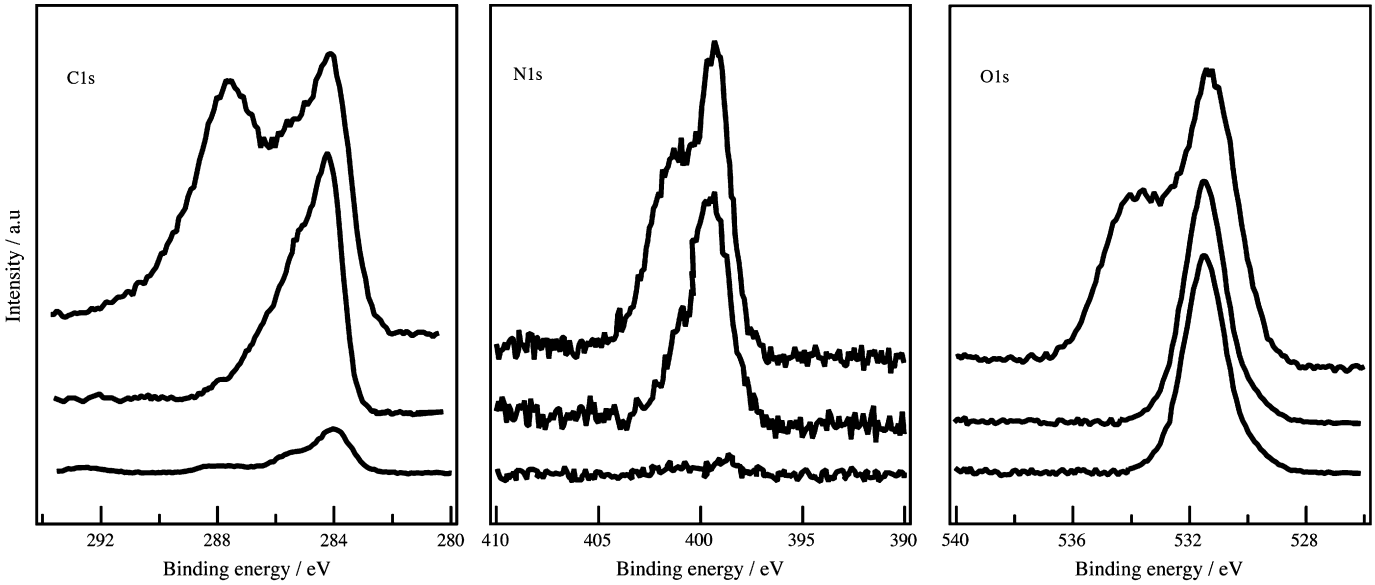

Fig. 2. C1s, N1s, and O1s XPS spectra for (a) SiO_2-coated crystal, (b) APTES-modified crystal, and (c) PNIPAm-modified crystal.

medium, respectively. The dissipation response is given by [69,70]

$$\Delta D = 2(f_0/n)^{1/2}\left(\eta_1\rho_1/\pi\mu_q\rho_q\right)^{1/2} \quad (4)$$

The frequency and dissipation response due to the grafting of the polymer chains on the surface of the quartz crystal can be obtained by removing the effects of the viscosity and density of water based on Eqs. (3) and (4). These values are subtracted from the corresponding Δf and ΔD for PNIPAm-grafted crystal to obtain the corrected Δf and ΔD for the grafted PNIPAm chains.

The temperature response of PNIPAm brushes was probed by QCM-D in two modes, in quasi-static mode and in real-time mode. In quasi-static mode, the response curve was collected at discrete temperature intervals. The sample was equilibrated at each temperature for 15 min before the data was collected. In real-time mode, the temperature of water was changed continuously at constant rate.

Fig. 3 shows the temperature dependence of frequency shift, Δf of PNIPAm brushes in single heating and cooling cycle in both quasi-static mode and real-time mode. The heating and cooling rates for real-time mode were 0.1 and 0.6 °C/min [71], respectively. In quasi-static mode the frequency shift, Δf gradually increases with increasing temperature in the heating process over the range 20–40 °C. Increase in Δf indicates a decrease in effective mass of the grafted PNIPAm attached to the crystal. At lower temperature, water is a good solvent for PNIPAm, therefore PNIPAm chains are in fully hydrated state. As the temperature increases, dehydration occurs and PNIPAm chains gradually collapse. Since the PNIPAm chains are chemically attached to the crystal, the observed decrease in mass is explained by the loss of hydrated water of PNIPAm chains. On the other hand, gradual decrease in Δf was observed with lowering temperature in the cooling process, which is due to the gradual hydration of PNIPAm chains.

The frequency shift, Δf obtained in real-time mode is similar to that obtained in quasi-static mode, except that the hysteresis observed in real-time mode is marginally less. We also examined the effects of heating and cooling rate on the kinetic process of coil-to-globule transition of polymer brushes and found that the hysteresis becomes smaller with increasing rate. These results may be due to the fact that the polymer brushes were kept in the collapsed state for shorter period compared with a quasi-static mode. Although it is difficult to compare the frequency shift, Δf obtained in two different modes, the similar characteristics of data obtained in real-time mode and in quasi-static mode indicate that the PNIPAm brush responds in real time to temperature changes imposed.

Fig. 4 shows the temperature dependence of the dissipation change, ΔD in a single heating–cooling cycle in both quasi-static mode and real-time mode simultaneously obtained with frequency shift Δf shown in Fig. 3. Dissipation of a viscoelastic polymer layer on quartz crystal is strongly influenced by its conformation. A dense or rigid layer has small dissipation energy, whereas a looser and more flexible layer has larger dissipation energy. The dissipation decreases with increasing temperature in the heating process, which indicates that PNIPAm brushes gradually collapse into compact conformation. In the cooling process, the dissipation increases with decreasing temperature over a temperature range from 40 to 20 °C, indicating that the collapsed brushes swell and become more flexible. It is worthy to mention that some characteristic points are observed in the heating and cooling processes. The heating process is characterized by three stages, and there exists a plateau region in ΔD indicated as stage II in Fig. 4. A ΔD value in the cooling process is larger than that in the heating process, whereas an opposite trend is observed for

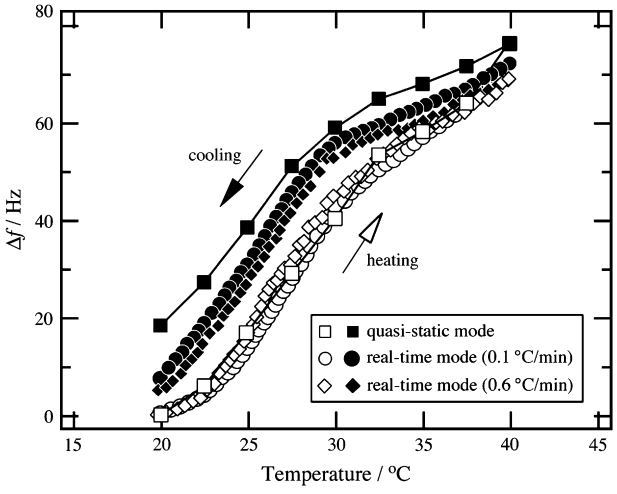

Fig. 3. Temperature dependence of frequency shift, Δf for PNIPAm brushes at $n = 7$. In the quasi-static mode (□, ■), the sample was equilibrated at every temperature for 15 min before the data was collected. In real-time mode, the heating and cooling rate was 0.1 °C/min (○, ●) and 0.6 °C/min (◇, ◆). Open and closed symbols, respectively, indicate heating and cooling process for both modes.

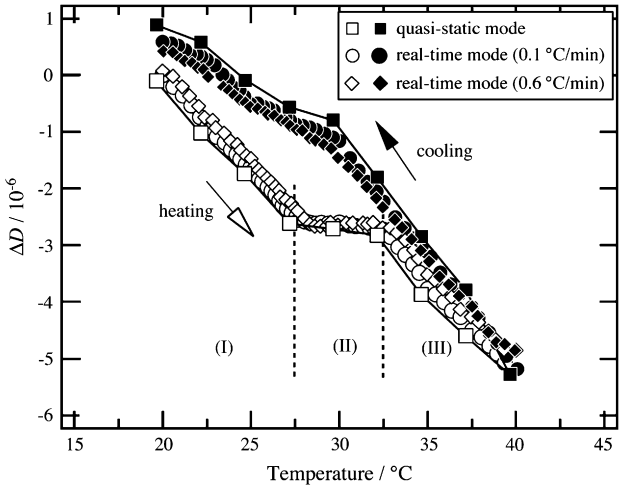

Fig. 4. Temperature dependence of dissipation shift (ΔD) for PNIPAm brushes at $n = 7$ in real-time mode. In quasi-static mode (□, ■), the sample was equilibrated at every temperature for 15 min before the data was collected. In real-time mode, the heating and cooling rate was 0.1 °C/min (○, ●) and 0.6 °C/min (◇, ◆), respectively. Open and closed symbols, respectively, indicate heating and cooling process for both modes.

Δf as shown in Fig. 3. This may be related to the characteristics of the outer layer of the PNIPAm brushes. As with the frequency shift, Δf, the hysteresis observed in real-time mode is less than that observed in quasi-static mode. In real-time mode, the polymer brushes were kept in the collapsed state for shorter period compared with a quasi-static mode.

Fig. 5a and b display the temperature dependence of frequency shift, Δf and dissipation change, ΔD of PNIPAm brushes in single heating and cooling cycle over a temperature range of 15–50 °C in quasi-static mode. For comparison, Δf and ΔD of PNIPAm brushes obtained by measurement over a narrow range of temperature (20–40 °C) shown in Figs. 3 and 4 are also plotted. The frequency shift, Δf and the dissipation change, ΔD obtained from both temperature ranges are similar except that the hysteresis observed by the measurement over a broader range of temperature (15–50 °C) is larger. The hysteresis is time dependent with difference when the polymer is kept in the collapsed state for a long time. To reveal the detailed temperature-dependent conformational change of PNIPAm chain, systematic study of the effect of two critical brush parameters, the surface density and molecular weight is needed.

3.4. Conformational change in PNIPAm brushes

The results obtained by QCM-D clearly reveal that there exist three kinetic steps in heating process. When $T < 27.5$ °C, ΔD decreases with increasing Δf, indicating that the shrinking and dehydration of PNIPAm chains occur simultaneously. The freely mobile grafted chains, which were expected to show the rapid dehydration, make densely packed brushes on the outer layer with increasing temperature. Formation of a dense and anchored outer layer leads to the decrease in ΔD as observed in stage I. In the temperature range $27.5 < T < 32.5$ °C, there exists a plateau region in ΔD despite the fact that Δf increases. In this range, since a dense, collapsed PNIPAm layer impermeable to water is formed in the outer layer, the shrinking of PNIPAm chains is limited by suppressed water permeation from the interior through the dense outer layer, which gives rise to the plateau region in temperature dependence of ΔD as observed in stage II, shown in Fig. 4. Some of the dehydrated water is trapped in the dense polymer brushes, and the trapped water gradually diffuse out of the brushes with increasing temperature, which leads to a frequency shift. Further heating makes the polymer brushes collapse, leading to increase in Δf and decrease in ΔD at 32.5 °C $< T$.

In the cooling, two kinetic steps are identified. In the temperature region from 40 to 27.5 °C, rapid increase in ΔD is observed accompanied by decrease in Δf, suggesting that PNIPAm chains of outer layer of the brushes are hydrated and become flexible. The brushes begin to swell from the outer layer to inner core. At the initial stage of cooling process, therefore, the random and flexible short chains give rise to an increase in ΔD. Since the amount of water bound to PNIPAm chains is still limited in this stage, decrease in Δf is small. When $T < 27.5$ °C, the change in ΔD becomes smaller against the variation of Δf. This is probably because polymer brushes close to the crystal surface is constrained by the intra- and interchain interactions formed in the collapsed state. Such interactions hinder the hydration of the collapsed chains in the cooling process. Therefore the change in the frequency Δf is mainly caused by hydration and dehydration, whereas the change in the dissipation ΔD is due to the conformational change.

It should be noted that the changes in frequency and dissipation during both heating and cooling processes are continuous in contrast to the sharp coil-to-globule transition observed for free PNIPAm chains in dilute solution. Zhulina et al. [20]

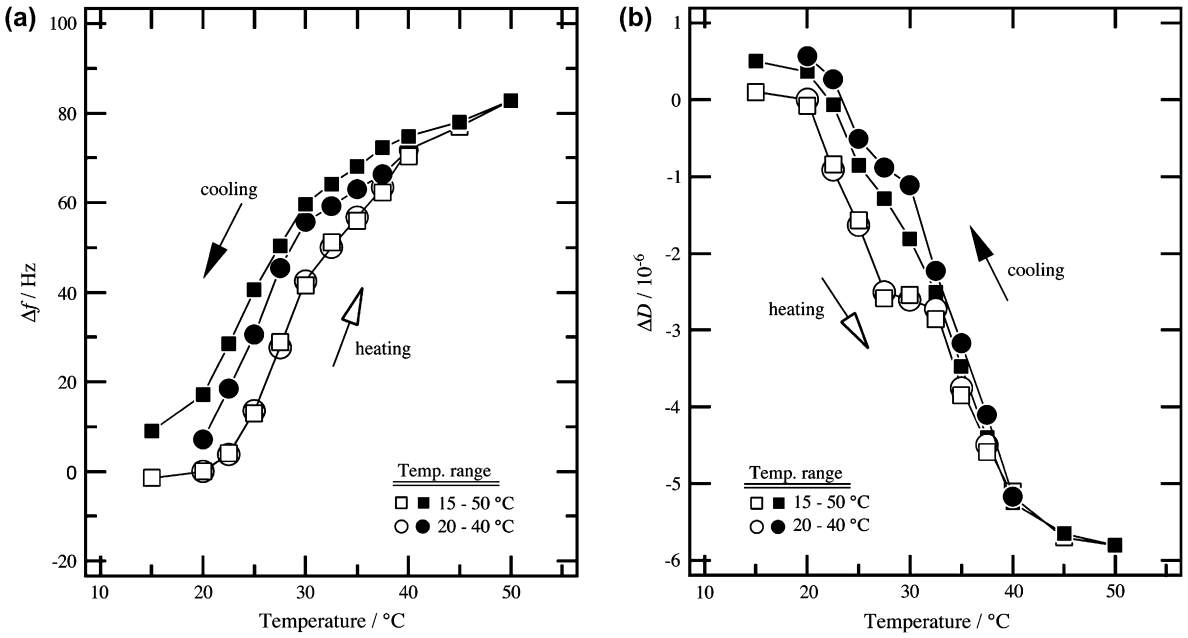

Fig. 5. The temperature dependence of (a) frequency shift, Δf and (b) dissipation change, ΔD of PNIPAm brushes in single heating and cooling cycle over a temperature range of 15–50 °C in quasi-static mode (□, ■). For comparison, Δf and ΔD of PNIPAm brushes obtained by measurement over a narrow range of temperature (20–40 °C) (○, ●) shown in Figs. 3 and 4 are also plotted.

and Birshtein et al. [21] developed the mean-field analytical theory describing the conformational transition related to the collapse of the layers of polymer chains grafted onto the impermeable surface of different morphologies. It is shown that in the case of a planar surface this transition is not a true thermodynamic phase transition. The reason for this is strong interchain interaction under the condition of dense grafting onto a plane. The interchain interaction in a layer makes the collapse transition weaker than in an isolated three-dimensional chain: the shift of the transition point to temperature below the Θ-temperature increases and the temperature range of the transition becomes broader. The most precise investigation of the structural characteristics was made for a planar layer on the basis of an analytical mean-field theory, which makes it possible to take into account the distributions of chain ends, the local chain stretching, and the concentration gradient in a layer. It is shown that at any solvent strength the planar layer of grafted polymer chains is inhomogeneous as a whole. The profile of unit density in the layer is described by a monotonically decreasing function, and the characteristic scale of density decrease coincides with the entire layer height. The stretching is inhomogeneous within each chain and different for different chains, and their ends are distributed throughout the layer. The observed behavior in accordance with the theoretical prediction, and transition occurs such that the polymer layer thickness decreases smoothly as solvent is excluded from the interfacial segments [20,33]. This continuous change arises from the high density and nonuniformity of the chains, which leads to broaden the transition and enlarge the hysteresis [20].

4. Conclusion

By using quartz crystal microbalance with dissipation monitoring, the phase behavior of poly(*N*-isopropylacrylamide) (PNIPAm) polymer brushes in water was observed at various temperatures in real-time mode. PNIPAm brushes exhibit a continuous change in conformation over the temperature range of 15–50 °C accompanied with large hysteresis, which reflects the gradual changes in frequency and dissipation. This result is in accordance with theoretical predictions that have suggested that polymer brush structure on planar surface do not exhibit true critical solubility transitions. This continuous change arises not only from intra- and interchain interactions formed in the collapsed state, but also from the high density and nonuniformity of the chains, which leads to broadening of the transition and thus enlarge the hysteresis.

Although QCM-D is a useful technique to follow the hydration transition of thermosensitive polymer brushes, more extensive study is needed to identify the microscopic structure for the complete understanding of the conformational changes of polymer brushes accompanied by a coil-to-globule transition. Two critical brush parameters, the surface density and molecular weight are considered to greatly affect PNIPAm chain conformation. To resolve this, neutron refractivity experiments exploring the temperature dependence of conformational change of PNIPAm chains prepared by living radical polymerization with good control over brush thickness and polydispersity and surface density are currently underway and will be reported in a future publication.

Acknowledgements

The work was partly supported by the R&D project for Environmental Nanotechnology of the Ministry of the Environment (MOE), Japanese government. MA acknowledges the Tokuyama Science Foundation for financial support.

References

[1] Taunton HJ, Toprakcioglu C, Fetters LJ, Klein J. Nature 1988;332:712.
[2] Taunton HJ, Toprakcioglu C, Fetters LJ, Klein J. Macromolecules 1990;23:571.
[3] Klein J, Perahia D, Walburg S. Nature 1991;352:143.
[4] Klein J, Kamiyama Y, Yoshizawa H, Israelachvili JN, Fretters L, Pincus P. Macromolecules 1992;25:2062.
[5] Perahia D, Wiesler DG, Satija SK, Fretters J, Sinha SK, Milner ST. Phys Rev Lett 1994;72:100.
[6] Field J, Toprakcioglu C, Ball R, Stanley H, Dai L, Barford W, et al. Macromolecules 1992;25:434.
[7] Cosgrove T, Heath TG, Phipps JS, Richardson RM. Macromolecules 1991;24:94.
[8] Auroy P, Auvray L, Leger L. Phys Rev Lett 1991;66:719.
[9] Auroy P, Auvray L, Leger L. Macromolecules 1991;24:2523.
[10] Auroy P, Auvray L, Leger L. Macromolecules 1991;24:5158.
[11] Raphaël E, de Gennes PG. J Phys Chem 1992;96:4002.
[12] Ji H, de Gennes PG. Macromolecules 1993;26:520.
[13] Alexander S. J Phys (Paris) 1977;38:983.
[14] de Gennes PG. J Phys (Paris) 1976;37:1445.
[15] Raphaël E, Pincus P, Fredrickson GH. Macromolecules 1993;26:1996.
[16] Auboy M, di Mehlio JM, Raphaël E. Europhys Lett 1993;24:87.
[17] Auboy M, Brochard-Wyart F, Raphaël E. Macromolecules 1993;26:5885.
[18] Williams DRM. J Phys II France 1993;3:1313.
[19] Lai PY, Halperin A. Macromolecules 1992;25:6693.
[20] Zhulina EB, Borisov OV, Pryamitsyn VA, Birshtein TM. Macromolecules 1991;24:140.
[21] Birshtein TM, Amoskov V, Mercurieva A, Pryamitsyn V. Macromol Symp 1977;113:151.
[22] Wijmans CM, Zhulina EB, Fleer GJ. Macromolecules 1992;25:2657.
[23] Israëls R, Leermarks FAM, Fleer GJ, Zhulina EB. Macromolecules 1994;27:3249.
[24] Lai PY, Zhulina EB. Macromolecules 1992;25:5201.
[25] Murat M, Grest GS. Phys Rev Lett 1987;63:1074.
[26] Grest GS. Macromolecules 1994;27:418.
[27] Chakrabarti A, Nelson P, Toral R. J Chem Phys 1994;100:748.
[28] Dickman R, Anderson PE. J Chem Phys 1993;99:3112.
[29] Lai PY, Binder K. J Chem Phys 1992;97:586.
[30] de Gennes PG. Macromolecules 1980;13:1069.
[31] Halperin A, Tirrell M, Lodge TP. Adv Polym Sci 1991;100:31.
[32] Milner ST. Science 1991;251:905.
[33] Szleifer I, Cargnano MA. Adv Chem Phys 1996;94:165.
[34] Stuart MAC, Waajen FHWH, Cosgrove T, Vincent B, Crowley TL. Macromolecules 1984;17:1825.
[35] Hadziioannou G, Patel S, Granick S, Torrell M. J Am Chem Soc 1986;108:2869.
[36] Chevalier Y, Brunel S, Le Perchec P, Mosquet M, Guicquero JP. Prog Colloid Polym Sci 1997;105:66.
[37] Zhao B, Brittain WJ. Prog Polym Sci 2000;25:677.
[38] Gast AP. Langmuir 1996;12:4060.
[39] Habitcht J, Schmidt M, Ruhe J, Johannsmann D. Langmuir 1999; 15:2460.

[40] Auroy P, Auvary L. Macromolecules 1992;25:3134.
[41] Heskins M, Guillet JE, James E. J Macromol Sci Chem 1968;A2:1441.
[42] Schild HG. Prog Polym Sci 1992;17:163.
[43] Hirokawa Y, Tanaka T. J Chem Phys 1984;81:6379.
[44] Takei Y, Aoki T, Sanui K, Ogata N, Sakurai Y, Okano T. Macromolecules 1994;27:6163.
[45] Zhang J, Pelton R, Deng Y. Langmuir 1995;11:2301.
[46] Jones DM, Smith JR, Huck WTS, Alexander C. Adv Mater 2002; 14:1130.
[47] Kanazawa H, Yamamoto K, Matsushima Y, Takai N, Kikuchi A, Sakurai Y, et al. Anal Chem 1996;68:100.
[48] Kikuchi A, Okano T. In: Okano T, editor. Biorelated polymers and gels. New York: Academic Press; 1998. p. 1–28.
[49] Yakushiji T, Sakai K, Kikuchi A, Aoyagi T, Sakurai Y, Okano T. Anal Chem 1999;71:1125.
[50] Yoshizako K, Akiyama Y, Yamanaka H, Shinohara Y, Hasegawa Y, Carredano E, et al. Anal Chem 2002;74:4160.
[51] Yamanaka H, Yoshizako K, Akiyama Y, Sota H, Hasegawa Y, Kikuchi A, et al. Anal Chem 2003;75:1658.
[52] Yanama N, Okano T, Sakai H, Karikusa F, Sawasaki Y, Sakurai Y. Macromol Chem Rapid Commun 1990;11:571.
[53] Shimizu T, Yamato M, Isoi Y, Akutsu T, Setomaru T, Abe K, et al. Circ Res 2002;90:e40.
[54] Balamurugan S, Mendez S, Balamurugan SS, O'Brien MJ, Lopez GP. Langmuir 2003;19:2545.
[55] Yim H, Kent MS, Satija S, Mendez S, Balamurugan SS, Balamurugan S, et al. Phys Rev E 2005;72:051801.
[56] Yim H, Kent MS, Mendez S, Balamurugan SS, Balamurugan S, Lopez GP, et al. Macromolecules 2004;37:1994.
[57] Yim H, Kent MS, Huber DL, Satija S, Majeswski J, Smith GS. Macromolecules 2003;36:5244.
[58] Liu G, Cheng H, Yan L, Zhang G. J Phys Chem B 2005;109:22603.
[59] Zhang G. Macromolecules 2004;37:6553.
[60] Jhon YK, Bhat RR, Jeong C, Rojas OJ, Szleifer I, Genzer J. Macromol Rapid Commun 2006;27:697.
[61] Kidoaki S, Ohya S, Nakayama Y, Matsuda T. Langmuir 2001;17:2402.
[62] The molecular weight distribution of PNIPAm was estimated by gel permeation chromatography (GPC), using a TOSOH HLC-8220GPC apparatus with TSKgel Super HM-Mx 2 columns, in HPLC grade DMF with 10 mM LiBr used as the mobile phase at a flow rate of 0.4 mL/min at 40 °C. Calibration was carried out with monodisperse poly(ethylene glycol) standards purchased from TOSOH Corp.
[63] Rodahl M, Höök F, Krozer A, Kasemo B, Brezinsky P. Rev Sci Instrum 1995;66:3924.
[64] Voinova MV, Rohdal M, Jonson M, Kasemo P. Phys Scr 1999;59:391.
[65] Sauerbery G. Z Phys 1959;155:206.
[66] Bottom VE. Introduction to quartz crystal unit design. New York: Van Nostrand Reinhold Co.; 1982.
[67] Liu G, Zhang G. J Phys Chem B 2005;109:743.
[68] Caruso F, Furlong DN, Kingshott P. J Colloid Interface Sci 1997;186:129.
[69] Höök F, Rodahl M, Brezinsky P, Kasemo B. Proc Natl Acad Sci USA 1998;95:12271.
[70] Höök F, Kasemo B, Nylander T, Fant C, Scott K, Elwing H. Anal Chem 2001;73:5796.
[71] In this study, our temperature-control system cannot achieve the linear response of temperature in cooling process above the cooling rate 1.0 °C/min, therefore we have chosen heating/cooling rate of 0.6 °C/min.